



Local compression process avoiding toughness change

A. Takumi Ozawa¹ · B. Hiroaki Kosuge² · C. Yoshiki Mikami³ · D. Tomoya Kawabata²

Received: 19 October 2021 / Accepted: 19 September 2022 / Published online: 19 October 2022
© International Institute of Welding 2022

Abstract

The local compression technique is used to achieve a straight crack front in weld specimens. However, some interested parties have reported that it decreases the fracture toughness value. The authors investigated the better local compression condition for securing a straight crack front while maintaining the fracture toughness value by a numerical analysis, and as a result, some local compression conditions, which do not involve compression of the crack tip, identified as promising. Fracture toughness tests were also conducted with these local compressions, and the test results showed that the fatigue precrack shape and fracture toughness value follows those estimated tendency by the numerical analysis. Two local compression conditions, which compress at the future notch side and ligament side by a square jig and at the ligament side by a circle jig, achieved a straight crack front while maintaining the fracture toughness value. The authors concluded that these new techniques are superior to that recommended in ISO 15,653.

Keywords Local compression technique · Weld specimens · Fracture toughness value

1 Introduction

High-end steels, represented by high strength steels such as 950 MPa class and 780 MPa class tensile strength and 460 MPa class yield stress steels, are increasingly applied to steel structures [1–4]. In many cases, safety evaluations for brittle fracture in welded joints are based on the crack tip opening displacement (CTOD) toughness in ISO 15,653:2018 [5], which provides a method of test

for the determination of quasistatic fracture toughness of welds. Section 12.3.3 of that standard requires precrack straightness, stating that “none of the seven interior crack length measurements shall differ from the weighted nine-point average value by more than $0.2 a_0$.” In addition, ISO 12,135:2016 [6], which provides a unified method of test for the determination of quasistatic fracture toughness, requires a minimum fatigue crack length in Section 5.5.2, which states that “The minimum fatigue crack extension shall be the larger of 1.3 mm or 2.5% of the specimen width.” Although base material specimens often meet these requirements without the use of special techniques, weld specimens often do not due to poor crack growth at mid-thickness unless special techniques are applied. The cause has been considered to be a complex residual stress distribution through the specimen thickness. It has also been reported that an elevated value of fracture toughness may be obtained with a bowed crack front shape [7]. In order to achieve a straight crack front, local compression (LC) is recommended in Annex C to ISO 15,653:2018 [5]. Annex C recommends application of LC within the notch tip to produce a total plastic strain of up to 1% of the specimen thickness. Although this technique has been used widely, some interested parties have reported that it results in an excessive underestimation of CTOD toughness [8, 9], and ISO 15,653 also mentions the effect of LC on fracture

Recommended for publication by Commission X—Structural Performances of Welded Joints—Fracture Avoidance.

✉ A. Takumi Ozawa
ozawa-t@m.mpat.go.jp

B. Hiroaki Kosuge
kosugefract@gmail.com

C. Yoshiki Mikami
mikami@jwri.osaka-u.ac.jp

D. Tomoya Kawabata
kawabata@fract.t.u-tokyo.ac.jp

- ¹ National Maritime Research Institute, 6-38-1 Shinkawa, Mitaka, Tokyo, Japan
- ² Graduate School of Engineering, The University of Tokyo, 7-3-1, Hongo, Bunkyo, Tokyo, Japan
- ³ Joining and Welding Research Institute, Osaka University, 11-1 Mihogaoka, Ibaraki, Osaka, Japan

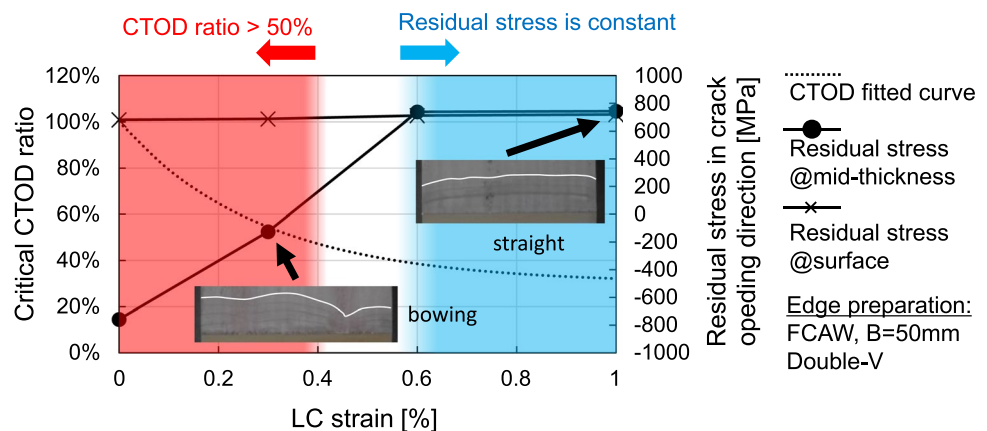
toughness. While excessive underestimation is not a significant problem for structural safety, not only safety but also rational evaluation has been required recently from the viewpoints of the environment and economy. For example, excessive underestimation may unreasonably prevent application of the above-mentioned new materials, which are useful in the environmental and economic aspects.

Based on the above, the authors investigated the typical effect of LC on crack front straightness and fracture toughness in a previous study [10]. Figure 1 shows a representative result. The numerical analysis in that study showed that, LC strain of 0.6% or more is required in order to relax the complex welding residual stress distribution. On the other hand, the results of a sacrificial test showed that 0.3% LC strain is insufficient to secure a straight crack front. However, the fracture toughness test results showed that the critical CTOD had already decreased by half at 0.4% LC strain. These various results indicate that it is difficult to maintain both fracture toughness and crack front straightness only by adjusting the amount of LC strain.

2 Purpose of this study

Based on the above-mentioned background, the authors investigated a new LC process which is capable of achieving a straight crack front while also maintaining fracture toughness. The required load was also considered. Since the load capacity of most general testing machines is 1 000 kN, we also considered whether the required load was within the typical 1 000 kN capacity or exceeded the limit of the testing machine. Previous studies [8–10] show LC decrease the fracture toughness evaluation value; however, no useful research results have been obtained for a concrete LC condition that replaces the current recommended conditions in ISO 15,653 for securing a straight crack while also maintaining fracture toughness. This study provide it and attempt to contribute reasonable safety assessment in unstable fracture.

Fig. 1 Critical CTOD and residual stress [10]

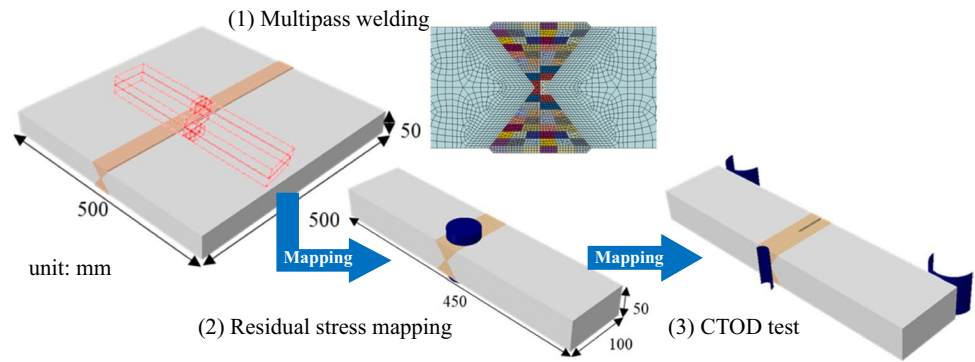


3 Numerical analysis

3.1 Through process modelling of local compression

In order to simulate the welding and LC processes, the authors conducted a finite element analysis to newly proposed LC conditions by the same method as in a previous study [10, 11]. Figure 2 shows the overview. First, a welding process simulation was performed on a welded joint with a 500 mm length, 500 mm width, and 50 mm thickness. The multilayer welding comprises 60 passes with an X-shaped groove and is simulated by a sequentially coupled finite element analysis of heat transfer and thermoelastic plasticity using the general-purpose finite element analysis software Abaqus. The actual residual stress distribution would depend on the groove geometry and welding technique employed. In this study, welding process in X-shaped groove joint with flux cored arc welding was simulated taking into account of generality and symmetry. In addition, the aim of this analysis is to simulate the residual stress, and change in physical properties in heat-affected zone (HAZ) region is not taken into consideration since it is assumed that a machined notch is introduced in the center of the weld metal. However, the authors are of the view that this method is applicable to the failure in HAZ region if the change is considered. Following the welding process simulation, a specimen with a 500 mm length, 100 mm width, and 50 mm thickness is extracted, and LC is applied simultaneously to both faces. After LC, a crack with a length of 50 mm, consisting of a 44 mm machined notch and a 6 mm fatigue precrack, is made in the specimen. The machined notch meets the related requirement in ISO 12,135. In this analysis, the authors used constitutive equations for different materials with a mixed hardening law for the elements in the base material and weld metal determined from the monotonic tensile test results of the base material and weld metal, under the rational assumption that the back stress value saturates

Fig. 2 Overview of finite element simulation of LC after multi-pass welding



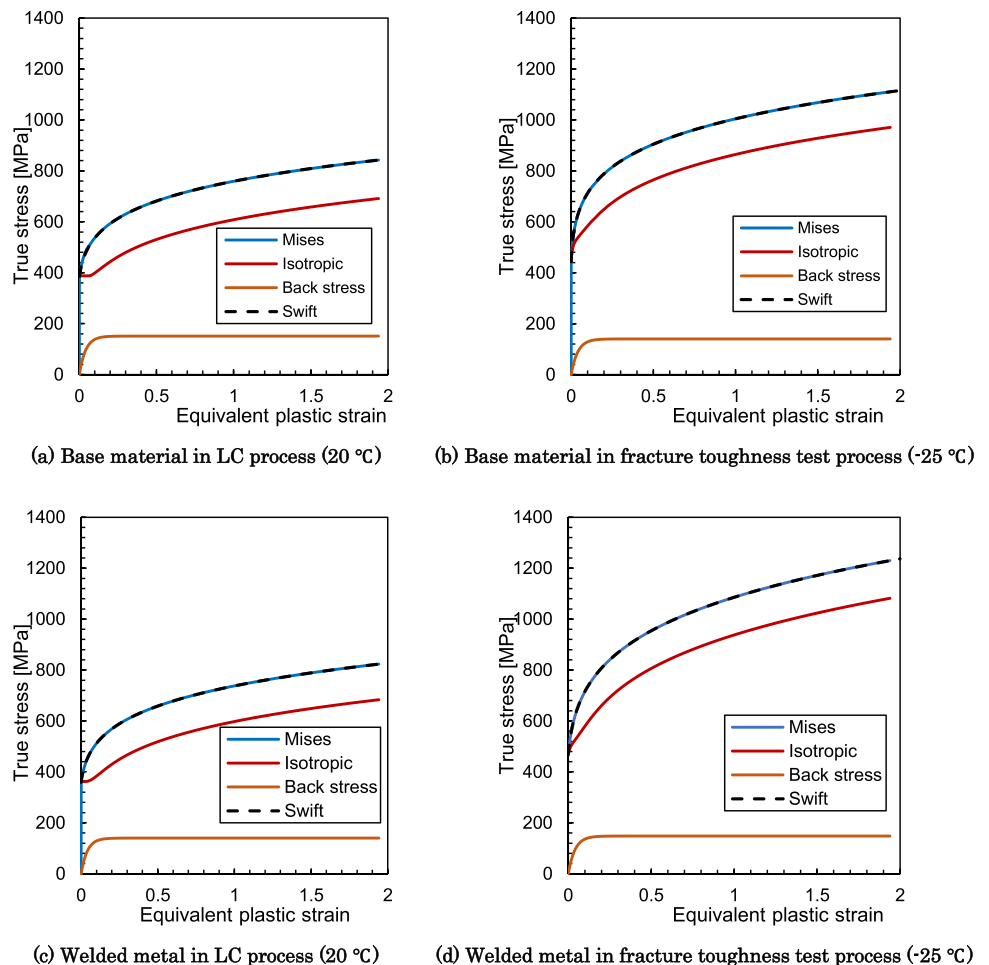
to the same constant value and no isotropic component is included in the early stage of plastic deformation. Figure 3 shows the stress–strain curves and their breakdown for the isotropic and kinematic components.

3.2 Fracture toughness simulation

Kawabata et al. proposed a fracture toughness test simulation process which faithfully reproduces the experiment

[12]. The authors carried out the fracture toughness test simulation according to that process and obtained the Weibull stress from the analysis results. The Weibull stress was used as the fracture criterion based on reports by some parties [13, 14]. In this study, the value of Weibull’s shape parameter was set to 20 based on the result of a numerical analysis with the same material. Figure 4 shows the process for estimating the fracture point using the Weibull stress. The fracture point is decided from the Weibull

Fig. 3 Stress–strain curves used in numerical analysis



stress of the as-welded specimen model. LC is not applied to this model. Only the result of plastic strain is imported, and the stress from the welding process simulation is not imported. The Weibull stress is regarded as the fracture point when the critical CTOD of this model calculated in accordance with ISO 15,653 [5, 15–17] reaches 0.1 mm and the value of the Weibull stress is about 1 800 MPa. In Fig. 4, the critical CTOD of the specimen to which LC-1 was applied is regarded as about 0.06 mm, and that of LC-2 is about 0.13 mm. Thus, from the viewpoint of maintaining the critical CTOD evaluation value, a LC process in which the critical CTOD is near 0.1 mm at Weibull stress of 1 800 MPa is desirable.

3.3 Search for better LC conditions

Based on the above-mentioned numerical analysis results, the authors attempted to identify candidate LC conditions

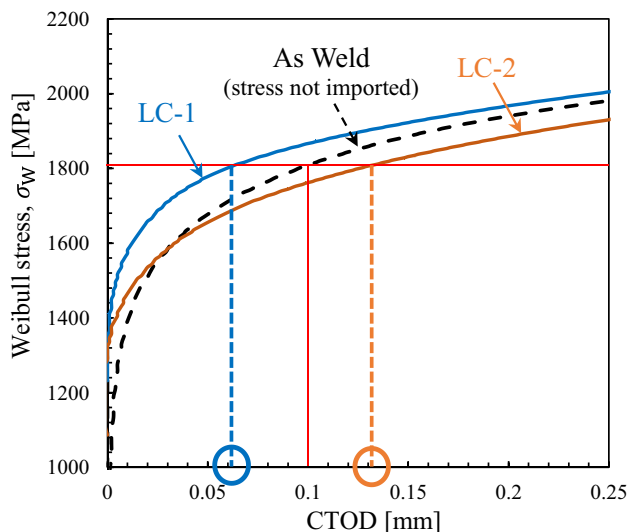
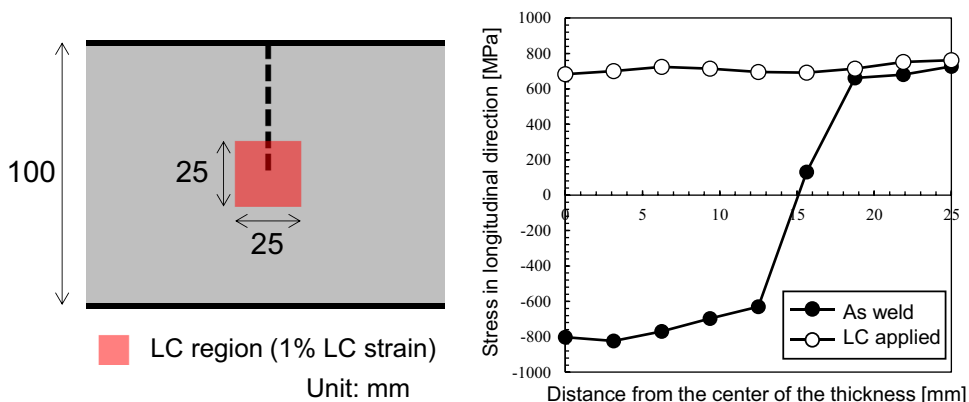


Fig. 4 Estimation of critical CTOD after LC using Weibull stress criterion

Fig. 5 LC process and welding residual stress in Square C



for achieving a straight crack front while also maintaining the critical CTOD. With regard to crack front straightness, the authors considered that the fatigue precrack grows in a straight line when the residual stress is positive and is evenly distributed through the specimen thickness. The examples explored in this study are described in the following sections.

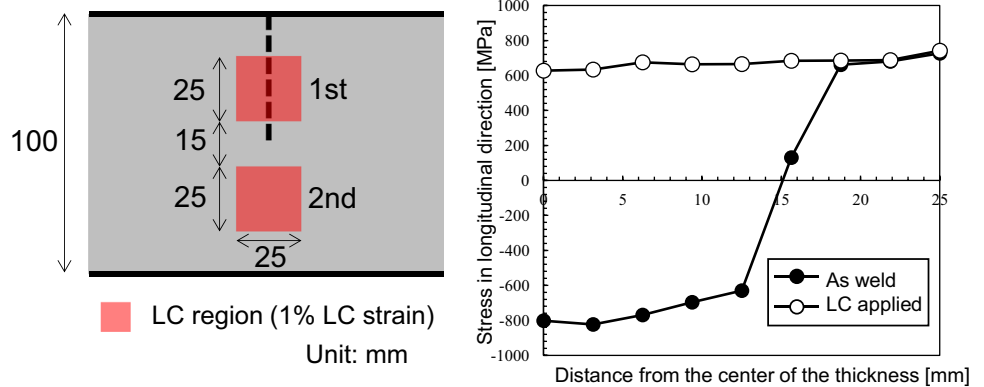
3.3.1 Square C

Figure 5 shows the LC process and the longitudinal residual stress distribution through the specimen thickness. This LC process is applied to the future notch tip like recommended in the ISO recommended one. This LC process is referred to hereinafter as “Square C,” where “C” means center. In this LC process, the specimen is compressed at the center of the future notch tip by a square jig with a side length of 25 mm until LC strain reaches 1%. This LC sufficiently relaxes the residual stress, as shown in Fig. 5, and the required load is estimated to be about 840 kN, which is sufficiently lower than the load limit of 1 000 kN. This LC is one of the most widely used processes and is known to achieve a straight crack front. However, the critical CTOD evaluation value decreases to 0.059 mm, which is about 60% of the original value of 0.1 mm. Thus, this traditional LC technique can secure a straight crack front, but the critical CTOD evaluation value may be underestimated significantly. This result is qualitatively consistent with the experimental results of our previous study [10].

3.3.2 Square N-L

Figure 6 shows the proposed square LC process and the longitudinal residual stress distribution through the thickness. In the following, this process is referred to hereinafter as “Square N-L,” where “N” means notch and “L” means ligament. In this LC process, the specimen is compressed at the future notch side and ligament side by a square jig with a side length of 25 mm until LC strain reaches 1%. The

Fig. 6 LC process and welding residual stress in Square N-L

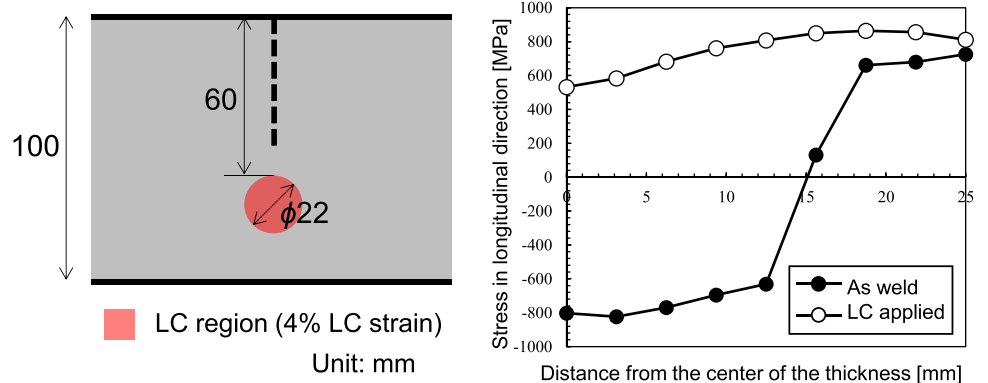


residual stress is relaxed sufficiently, as shown in Fig. 6, and the required load is estimated to be about 820 kN, which is sufficiently lower than 1 000 kN. Unlike the traditional LC, the notch tip is not compressed. The critical CTOD evaluation value is 0.141 mm, which is higher than the original 0.1 mm. Therefore, this LC can achieve a straight crack front, and the critical CTOD evaluation value may be overestimated slightly.

3.3.3 Circle L

Figure 7 shows the proposed circle LC process and the longitudinal residual stress distribution through the thickness. This LC process is referred to hereinafter as “Circle L.” Here, the specimen is compressed at the ligament side by a circle jig with a diameter of 22 mm until LC strain reaches 4%. The residual stress is relaxed sufficiently, as shown in Fig. 6, and the required load is estimated to be about 750 kN, which is sufficiently lower than 1 000 kN. As in Square N-L, the notch tip is not compressed. The critical CTOD evaluation value is 0.145 mm, which is higher than the original 0.1 mm. Therefore, this LC can achieve a straight crack front, but the critical CTOD evaluation value may be overestimated.

Fig. 7 LC process and welding residual stress in Circle L



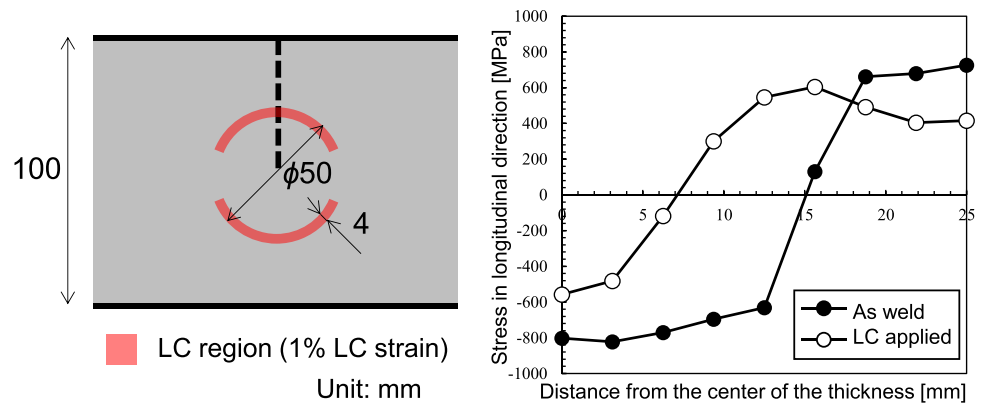
3.3.4 Ring C

Figure 8 shows the proposed LC process with ring jig and the longitudinal residual stress distribution through the thickness. This process is referred to hereinafter as “Ring C.” In this LC process, the specimen is compressed around the notch tip using a deficient ring jig with an outer diameter of 50 mm and a thickness of 4 mm until LC strain reaches 1%. Since the critical CTOD evaluation value is estimated at 0.094 mm, which is near the original 0.1 mm, this LC process has the advantage of maintaining the critical CTOD. However, the residual stress is not relaxed sufficiently by 1% LC strain, as shown in Fig. 8. To relax the residual stress, it is necessary to apply a higher LC strain, but in this case, the required load reaches about 950 kN, which is near to the load limitation of 1 000 kN. While it would be possible to apply higher LC strain to a specimen with the ideal shape, application of higher LC strain cannot be guaranteed with actual specimens because real specimens have surface asperities.

3.3.5 Summary of identified LC conditions

Figure 9 shows the residual stress at mid-thickness in longitudinal direction and critical CTOD evaluation value for each

Fig. 8 LC process and welding residual stress in Ring C



identified LC condition. Considering the fact that the residual stress in Fig. 8 was uniformly distributed or the minimum value was at the mid-thickness position, the longitudinal residual stress at mid-thickness is used for the horizontal axis. In order to maintain the critical CTOD evaluation value, the value must be within a certain range from 0.1 mm, as indicated by the blue region in Fig. 9, and to achieve a straight crack front, the residual stress must be tensile, as in the red region in the figure. Based on these conditions, the authors estimated that the better LC condition is within the region surrounded by the dotted line in Fig. 9.

4 Fracture toughness test

4.1 General

In order to verify the new LC process obtained by the numerical analysis, the authors conducted an actual fracture toughness test with the new LC process conditions. The base material and welding material were the same as those used in the previous study [10], that is, EH40 [18] and DW-Z100

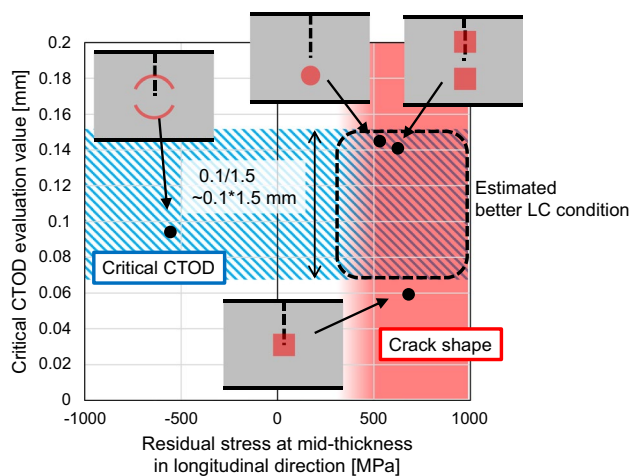


Fig. 9 Residual stress and critical CTOD for identified LC conditions

(AWS No: A5.20 E71T-1C). After cutting a sample with a 450 length, 100 mm width, and 50 mm thickness from the welded joint, LC was applied with the same as that obtained by the numerical analysis. Next, a machined notch with a length of 44 mm and a fatigue precrack with a length of 6 mm was introduced, and a fracture toughness test was conducted. Table 1 shows the test conditions. The number of tests was 5 for each LC condition, and the test temperature was $-25\text{ }^{\circ}\text{C}$. With the Ring C process, in addition to the test with 1% LC strain, 1.5% LC strain was also applied considering the poor welding residual stress relaxation observed with 1% strain in the numerical analysis. The groove geometry and an image of the macro section are shown in Fig. 10. Such multi-pass welded thick structural steel is a typical welded joint for which LC is applied because it is difficult to achieve straight precrack due to a high and complex residual stress distribution.

4.2 Test results

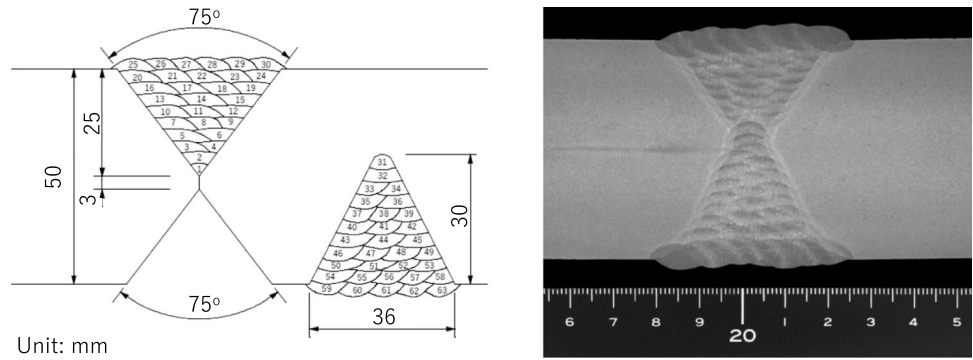
4.2.1 LC process

Almost all specimens reached an amount of LC strain near the target value. However, in the Ring C with the target LC strain of 1.5%, a specimen did not reach the target LC strain even at the testing machine load limit of 1 000 kN. As mentioned in Section 3.3.5, a load of around 1 000 kN is required in order to reach the target LC strain, and some specimens may not reach the target due to surface asperity.

Table 1 Test conditions

LC	Target LC strain	Number of specimens	Test temperature
Square C	1%	5	$-25\text{ }^{\circ}\text{C}$
Square N-L	1%	5	$-25\text{ }^{\circ}\text{C}$
Circle L	4%	5	$-25\text{ }^{\circ}\text{C}$
Ring C	1%	5	$-25\text{ }^{\circ}\text{C}$
Ring C	1.5%	5	$-25\text{ }^{\circ}\text{C}$

Fig. 10 Groove geometry and macrosection



4.2.2 Fracture toughness test

Figure 11 shows representative fractographs for each LC condition. In Fig. 11, the fatigue crack fronts are highlighted in red line. In all tests, stable crack growth and the ductile fracture surface were hardly observed, and a brittle fracture surface was observed immediately after the fatigue precrack. Except for the Ring C LC condition, the fatigue precracks grew in a straight line, and all specimens met requirements for straightness of the fatigue precrack in ISO 12,135 and 15,653. However, the fatigue precracks of Ring C were bowed, and 4 of the 5 specimens did not meet the straightness requirement due to poor fatigue crack growth at mid-thickness. As mentioned in Section 3.3.5, poor residual stress relaxation is concerned with Ring C LC, and in actuality, the

fatigue precracks were bowed. Therefore, the authors are of the view that estimation of the fatigue precrack straightness from the amount of residual stress relaxation is an effective approach. In Ring C LC, the fatigue precrack was bowed, but straightness could be improved by increasing the LC strain, suggesting that Ring C LC may be an effective method if larger LC strain is applied to a smaller specimen.

Figure 12 shows the critical CTOD for each LC condition obtained from the fracture toughness test. Black circle indicate valid results, X means an invalid result due to poor crack front straightness, and the red lines are the maximum likelihood estimate (MLE) of the scale parameter in Weibull distribution, which is used as a representative value of the critical CTOD and is obtained from the root mean square of the test results.

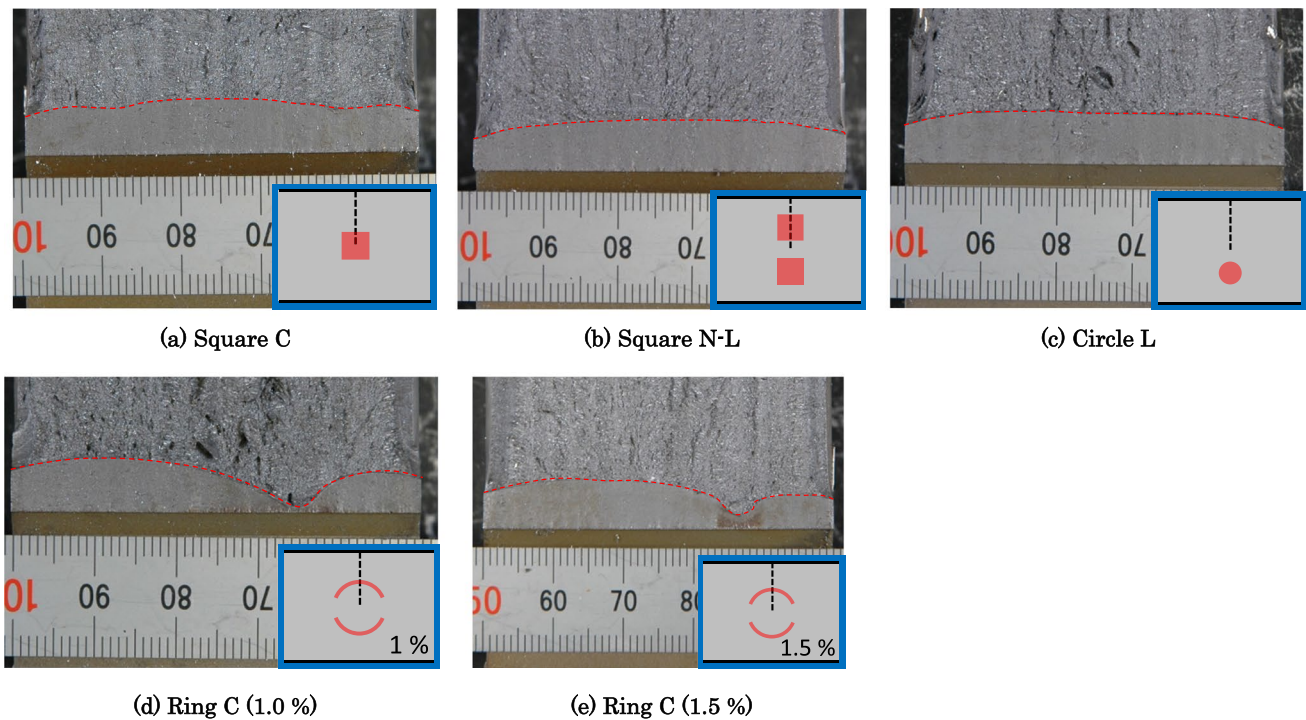


Fig. 11 Representative fractographs for each LC condition

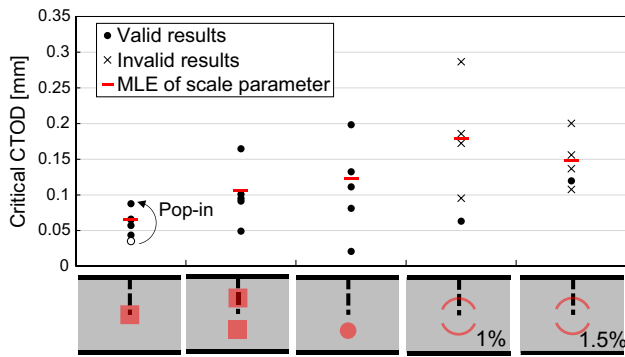


Fig. 12 Critical CTOD for each LC condition

The critical CTODs of Square N-L and Circle L are slightly less than twice that of Square C. Therefore, in the authors’ view, these new LC conditions are superior to traditional LC, considering the result of the previous study [10], which indicated that traditional LC decreases the critical CTOD by more than 50%. Although the numerical analysis in chapter 3 assumed that Square N-L and Circle L would overestimate fracture toughness, the estimates obtained by these processes were close to the true value. In this regard, it should be remembered that no factor other than the Weibull stress was considered in the fracture toughness estimation in the numerical analysis stage. Considering this, the authors are of the view that other factors, such as material deterioration due to plastic strain, also have an effect on fracture toughness in actual measurements.

The critical CTOD of Ring C was more than twice that of Square C. However, it should be noted that the fatigue precrack was bowed and 4 specimens did not meet the related requirements in ISO 12135.

The test results are summarized in Fig. 13, where the vertical axis is the critical CTOD and the horizontal axis

is the ratio of the minimum fatigue crack length to the specimen width. The fracture test meets the ISO 12,135 requirement for the minimum fatigue crack length when the value of the horizontal axis is more than 2.5%.

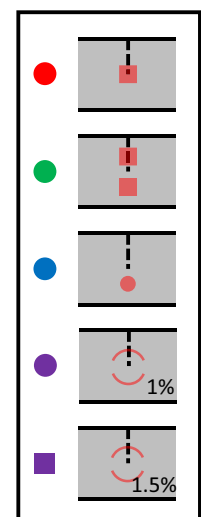
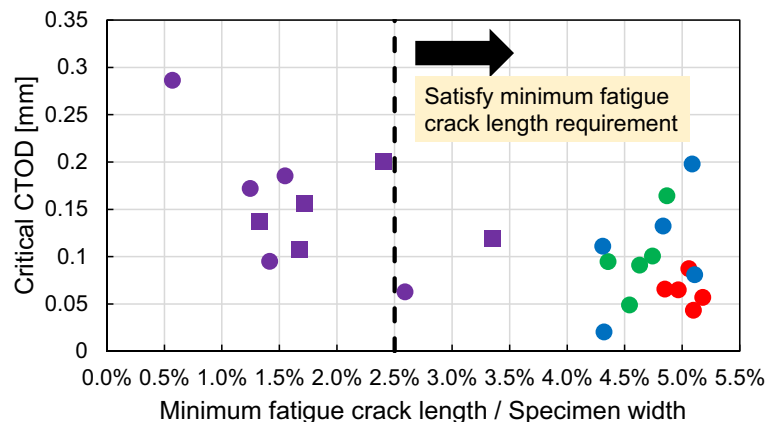
Pop-in occurred in all the fracture toughness tests using the traditional Square C method but did not occur in any of the other tests. Figure 14 shows a representative fracture surface caused by pop-in and the region where LC was applied in Square C. The dotted red line indicates the pop-in stop position. In Square C, all pop-in stopped in the LC region, and in some specimens, pop-in stopped at the border of the LC region. The authors believe that this is an interesting result, suggesting a possible candidate for the cause of the fracture toughness deterioration observed with traditional LC.

5 Conclusion

In order to search for the better LC condition, which achieve a straight crack front while maintaining the critical CTOD, the authors carried out:

- Numerical analysis for estimating the crack front shape and critical CTOD. Square N-L, Circle L, and Ring C conditions were identified as candidates for the better LC condition.
- Actual fracture toughness tests using these identified LC conditions. Square N-L and Circle L conditions achieved a sufficiently straight crack front and met the ISO requirement. In addition, an accurate evaluation of the critical CTOD close to the true value is possible with the proposed LC conditions based on our previous study and the numerical analysis results.

Fig. 13 Summary of fracture toughness test



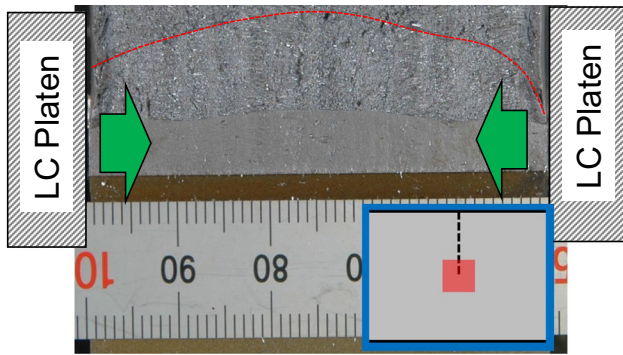


Fig. 14 Representative fracture surface by pop-in and LC region in Square C

As a result of this study, the authors concluded that the newly proposed Square N-L and Circle L conditions are the better LC condition than the traditional one.

Acknowledgements This study was carried out by the LCP Committee under the International Standard Development Project for Energy-Saving supported by the Nomura Research Institute, Ltd. and the Ministry of Economy, Trade and Industry. This work was also supported by JSPS KAKENHI Grant Number JP19H00802. Dr. Anai, Dr. Tsumura, and Mr. Ando provided generous cooperation in conducting the fracture toughness test. The authors are deeply grateful to all those concerned.

Declarations

Conflict of interest The authors declare no competing interests.

References

1. Japan Electric Power Civil Engineering Association (1992) One hundred years' history of hydropower plants (in Japanese). Japan Electric Power Civil Engineering Association, Tokyo
2. Kitada H, Fukui T (2014) New high-strength steel that makes a breakthrough in the marine field (in Japanese). Seizando, Tokyo
3. Hara N, Sugino T, Otsu M (2001) High-tough welding consumables for 950 N/mm² class high-strength steels. Kobe Steel Engineering Reports, vol 51
4. Sato M, Hara N (2009) Welding consumables for 780 and 950 MPa class high strength steels. J Japan Weld Soc 78(6):550–554
5. ISO15653:2018. Metallic materials – method of test for the determination of quasistatic fracture toughness of welds. ISO copyright office, Switzerland
6. ISO12135:2016. Metallic materials – unified method of test for the determination of quasistatic fracture toughness. ISO copyright office, Switzerland
7. Towers O, Daws M (1983) Welding Institute Research on the fatigue precracking of fracture toughness specimens. ASTM STP856. <https://doi.org/10.1520/stp34516s>
8. Meith WA, Hill MR, Panontin T (2001) Analytical and experimental study of fracture in bend specimens subjected to local compression. ASTM Fatigue and Fracture. <https://doi.org/10.1520/STP11087S>
9. Hara N, Sugino T, Otsu M (1999) Platen effects on fracture toughness of HT950 welds metal (in Japanese). Technical Papers of Welding Structure Symposium
10. Ozawa T et al (2021) Typical local compression effect on crack front straightness and fracture toughness. Weld World. <https://doi.org/10.1007/s40194-021-01119-x>
11. Mikami Y et al (2017) “Numerical simulation of residual stress modification by reverse bending of notched fracture toughness test specimens of multipass welds. Theoret Appl Fract Mech 92:214–222
12. Kawabata T et al. Applicability of local approach technique for the brittle crack initiation properties of prestrained steel plate,” to be submitted
13. Minami F (2006) Fracture assessment method using the Weibull stress – part I. Japan Weld Soc 75(5):416–446
14. Beremin (1983) A local criterion for cleavage fracture of a nuclear pressure vessel steel. Metall Trans A 14:2277–2287. <https://doi.org/10.1007/BF02663302>
15. Kawabata T et al (2016) Proposal for a new CTOD calculation formula. Eng Fract Mech 159:16–34
16. Kawabata T et al (2017) Plastic deformation behavior in SEB specimens with various crack length to width ratios. Eng Fract Mech 178:301–317
17. Kawabata T et al (2017) Applicability of new CTOD calculation formula to various a₀/W conditions and B×B configuration. Eng Fract Mech 179:375–390
18. (2019) Rules and guidance for the survey and construction of steel ships – part K Materials. ClassNK, ClassNK Information Center, Chiba

Publisher's note Springer Nature remains neutral with regard to jurisdictional claims in published maps and institutional affiliations.

Springer Nature or its licensor holds exclusive rights to this article under a publishing agreement with the author(s) or other rightsholder(s); author self-archiving of the accepted manuscript version of this article is solely governed by the terms of such publishing agreement and applicable law.